Iterative MMSE/MAP Impulsive Noise Reduction for OFDM

Paulo A. C. Lopes and José A. B. Gerald

Instituto de Engenharia de Sistemas e Computadores, Investigação e Desenvolvimento, Instituto Superior Técnico, Universidade de Lisboa, INESC-ID/IST/UL, Rua Alves Redol n.9, 1000-029 Lisbon, Portugal, paulo.lopes@tecnico.ulisboa.pt

Abstract

This paper proposes an iterative Minimum Mean Square Error (MMSE)/ Maximum A Posteriori (MAP) technique for impulsive noise reduction in telecommunications with Orthogonal Frequency Division Modulation (OFDM) modulation, its derivation and connection to previous works. Two versions of the technique are presented and compared with other works using Middleton class A noise and measured power lines noise. The technique starts by making an MMSE or MAP estimation of the received signal in the transform domain, and then it proceeds to make an MMSE estimate of the impulsive noise in the time domain. The estimate of the noise is then used to improve the estimate of the signal and this is done repeatedly.

Keywords: Impulsive Noise, Orthogonal Frequency Division Modulation (OFDM) , Noise Reduction, Iterative, Minimum Mean Squares Error (MMSE), Maximum A Posteriori (MAP)

1. Introduction

One type of noise that is common in communication systems is impulsive noise [1, 2, 3, 4]. The simplest methods for impulsive noise reduction in Orthogonal Frequency Division Modulation (OFDM) systems consist in clipping or nulling the impulses [5, 6, 7, 8]. Other methods are iterative [9, 10, 11] and others use more sophisticated techniques [12, 13, 14, 15, 16, 17]. Still, other methods use modifications of forward error correction coding [18, 19, 20].

In [9] Zhidkov et al. present an iterative technique where the transmitted signal is first estimated by demodulation (without removing the impulsive-noise) and then used to calculate an estimate of the received signal. This is then subtracted from received signal to obtain an estimate for the noise that allows the estimation of the impulses position using a threshold. These impulses are removed from the received signal and the transmitted signal is re-estimated. This is done iteratively. Haring et al. [10] present a more theoretical paper but related to the paper by Zhidkov as shown in the present paper. They use a general transform but this can be taken to be the discrete Fourier transform (DFT). Assuming this, they do impulsive noise estimates in the time domains and transmitted signal estimate in the transform domain, and iterate as in the Zhidkov paper. They use complex models for the noise in time and frequency domain. Chien et al. [13] use a similar technique to Zhidkov et al. but add channel estimation to the system. This is important because impulsive noise increases the difficulty of channel estimation.

Caire et al. [11] propose the use of compressed sensing to estimate the impulsive noise using pilot and null tones. They give rather restrict conditions on the number of impulses that can be detected using their method. In

[12] the author proposes to use the frequency domain correlation of the noise given the burst position to improve the data estimation, instead of trying to subtract the impulses in the time domain. Lin et al. [16] use sparse Bayesian learning (SBL) to estimate the impulsive noise using the pilot and nulls only and with data tones where the signal is taken as noise. They also develop an iterative technique that updates hiper-priors with noise estimates. Korki et al. [14] develop a hidden Markov model for burst/impulsive noise and a steep-descent algorithm to estimate this noise. This is done in conjunction with estimating parameters with SBL and a version of the Expectation Maximization (EM) algorithm. They estimate almost all the it's parameters from the data. Al et al. [17] simplify the impulsive noise Maximum Likelihood (ML) estimator by first estimating the impulse positions in time domain and then refining these estimates using ML and clusters. Finally, Nassar et al. [15] use a factor graph and belief propagation to estimate the channel bit and impulsive noise. They use a hidden Marcov model similar to Korki. They report an almost optimal demodulator with relatively low complexity.

2. Proposed Technique

This paper addresses the problem of determining a good demodulator for Quadrature Amplitude Modulation (QAM)/ Phase Shift Keying (PSK) OFDM signals in the presence of impulsive noise. The received signal $r(n)$ in the discrete time domain is taken to be formed by the transmitted signal $s(n)$ plus a Gaussian distributed random noise $g(n)$ and impulsive noise $i(n)$.

$$r(n) = s(n) + g(n) + i(n) \tag{1}$$

The goal is to estimate the impulsive noise component and remove it from the received signal. Designing an optimum minimum mean square error (MMSE) or maximum a posteriori (MAP) estimator for impulsive noise is a difficult task [10], but using an iterative solution to the problem seems promising. Here we follow the approach adopted by Haring [10] but reach a simpler result. In the derivation, a Middleton class A noise model is used [1, 2]. This type of noise is known to be a good fit for the noise in broadband Power Line Communication (PLC) channel [4, 3] although it can be improved for instance by adding memory to the model at the expense of an increase in the computational complexity. Periodic noise that is also common in PLC is not discussed in the work.

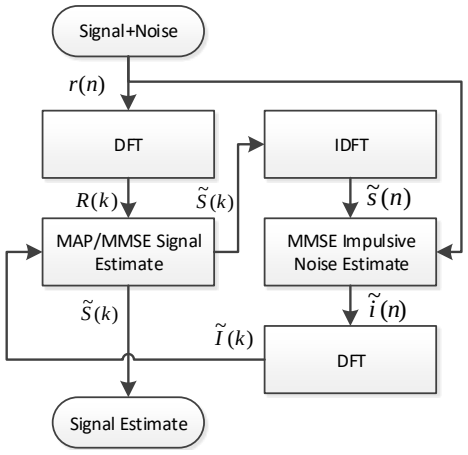

Figure 1: Flowchart of the proposed technique.

The proposed technique is presented in Fig. 1. First, the discrete Fourier transform (DFT) of the received signal is calculated, as in OFDM. Second, a MMSE or MAP estimation is done to estimate the received signal in the transform domain. Third, the signal estimate and the received signal are used

in a MMSE estimator to estimate the impulsive noise in the time domain. Finally, go back to second but using the impulsive noise estimate to improve the signal estimate. This is done repeatedly for a predetermined number of times. The signal estimate is obtained in the transform domain, like in a typical OFDM demodulator. The impulsive noise estimate is obtained in the time domain because this is where it is better distinguished from Gaussian noise.

3. Time Domain Impulsive Noise MMSE Estimate

First, the expression for the MMSE estimate of the impulsive noise given the received signal, $r(n)$, and the current estimate for the transmitted signal, $\tilde{s}(n)$, is determined. So we wish to calculate $P(i(n)|r(n), \tilde{s}(n))$; the probability that the random variable $i(n)$ takes the value $i_v(n)$ given that the random variables $r(n)$ and $\tilde{s}(n)$ take the values $r_v(n)$ and $\tilde{s}_v(n)$. Note that although these variables could be taken as random processes because they are considered independent in time (for instance $s(n_0)$ is independent of $s(n_1)$ for $n_0 \neq n_1$) they are better described by a simple set of random variables. Through the text the following notation is used: for any random variable x a sample from this random variable is x_v and $P(x \dots)$ always stands for $P(x = x_v \dots)$.

It is assumed that the current estimate for the transmitted signal is a Gaussian random variable, it is unbiased, and it has variance σ_s^2. The Gaussian assumption is justified by the central limit theorem [21, page 359] and by: 1) the time domain signal estimation error at any time slot is the sum of many independent estimation errors in the frequency domain (due to the

IDFT); 2) the transmitted signal at any time slot is the sum of many independent discrete uniform random variables (IDFT of a QAM signal). Note that transmitted signal estimate $\tilde{s}(n)$ is simply the sum of the transmitted signal $s(n)$ plus the transmitted signal estimation error. The Gaussian estimation errors will add to the Gaussian background noise, $g(n)$, resulting in a new Gaussian noise, $g'(n)$, with variance, $\sigma_{g'}^2 = \sigma_g^2 + \sigma_s^2$. Accordingly, we have, where the dependence on n was dropped

$$P(i|r,\tilde{s}) = \frac{P(i,r,\tilde{s})}{P(r,\tilde{s})} = \frac{P(i,r,\tilde{s})}{\int_{-\infty}^{\infty} P(i,r,\tilde{s})di_v}. \tag{2}$$

We also have

$$r(n) = \tilde{s}(n) + i(n) + g'(n). \tag{3}$$

$s(n)$, $i(n)$ and $g(n)$ are independent random variables. It will be assumed that $\tilde{s}(n)$, $i(n)$ and $g'(n)$ are also independent. Thus, we can write

$$P(i,r,\tilde{s}) = P(i,\tilde{s},g' = r_v - \tilde{s}_v - i_v) = P(i)P(\tilde{s})P(g' = r_v - \tilde{s}_v - i_v). \tag{4}$$

The first equality comes from the fact that the two events described are the same. The term $P(\tilde{s})$ does not depend on i_v so it will cut in the numerator and denominator of (2). The term $P(i)$ is the probability density function (PDF) of the impulsive Middleton class A noise [1, 2]. This is given by

$$P(i = i_v) = e^{-A}\delta(i_v) + \sum_{j=1}^{\infty} \frac{A^j e^{-A}}{j!} \mathrm{PDF_N}\left(i_v, 0, \frac{\sigma_i^2 j}{A}\right) \tag{5}$$

where $\mathrm{PDF_N}\left(x, m, \sigma^2\right)$ stands for the PDF of a real Gaussian variable and is given by

$$\mathrm{PDF_N}\left(x, m, \sigma^2\right) = \frac{1}{\sqrt{2\pi\sigma^2}} e^{-\frac{(x-m)^2}{2\sigma^2}} \tag{6}$$

and $\delta(x)$ stands for the Dirac delta. The term $P(g' = \dots)$ is given by

$$P(g' = r_v - \tilde{s}_v - i_v) = \mathrm{PDF_N}\left(r_v - \tilde{s}_v - i_v, 0, \sigma_{g'}^2\right). \tag{7}$$

The A term in (5) refers to the density of impulses and is usually much smaller than unit, $A \ll 1$, so that (5) can be approximated by using only the first term in the summation. This results in

$$P(i = i_v) = (1 - A)\delta(i_v) + A\ \mathrm{PDF_N}\left(i_v, 0, \sigma_{\mathrm{ix}}^2\right)\big) \tag{8}$$

with $\sigma_{\mathrm{ix}}^2 = \sigma_i^2/A$. This is also referred to as the Bernoulli Gaussian noise model [1].

Calculating (2) using (7) and (8) results in

$$P(i|r,\tilde{s}) = \frac{\left(\sigma_{g'}^2 + \sigma_{\mathrm{ix}}^2\right)\left((1-A)\delta\left(i_v\right) + \frac{Ae^{-\frac{i_v^2}{2\sigma_{\mathrm{ix}}^2}}}{\sqrt{2\pi}\sqrt{\sigma_{\mathrm{ix}}^2}}\right)e^{-\frac{i_v(2\tilde{s}_v + i_v - 2r_v)}{2\sigma_{g'}^2}}}{A\sqrt{\sigma_{\mathrm{ix}}^2}\sigma_{g'}^2\sqrt{\frac{1}{\sigma_{g'}^2} + \frac{1}{\sigma_{\mathrm{ix}}^2}}\exp\left(\frac{\sigma_{\mathrm{ix}}^2(r_v - \tilde{s}_v)^2}{2\sigma_{g'}^2\left(\sigma_{g'}^2 + \sigma_{\mathrm{ix}}^2\right)}\right) - A\sigma_{g'}^2 - A\sigma_{\mathrm{ix}}^2 + \sigma_{g'}^2 + \sigma_{\mathrm{ix}}^2} \tag{9}$$

The MMSE estimate of i will be given by

$$\tilde{i}_v = \mathrm{E}[i|r,\tilde{s}] = \int_{-\infty}^{\infty} i_v\, P(i|r,\tilde{s}) di_v. \tag{10}$$

Calculating the integral using (9) results in:

$$\begin{aligned}\tilde{i}_v = \mathrm{E}[i|r,\tilde{s}] = A\sqrt{\sigma_{\mathrm{ix}}^2}\left(r_v - \tilde{s}_v\right)\exp\left(\frac{\sigma_{\mathrm{ix}}^2\left(r_v - \tilde{s}_v\right)^2}{2\sigma_{g'}^2\left(\sigma_{g'}^2 + \sigma_{\mathrm{ix}}^2\right)}\right) \Big/ \\ \left(\sqrt{\frac{1}{\sigma_{g'}^2} + \frac{1}{\sigma_{\mathrm{ix}}^2}}\left(A\sqrt{\sigma_{\mathrm{ix}}^2}\sigma_{g'}^2\sqrt{\frac{1}{\sigma_{g'}^2} + \frac{1}{\sigma_{\mathrm{ix}}^2}}\exp\left(\frac{\sigma_{\mathrm{ix}}^2\left(r_v - \tilde{s}_v\right)^2}{2\sigma_{g'}^2\left(\sigma_{g'}^2 + \sigma_{\mathrm{ix}}^2\right)}\right)\right.\right. \\ \left.\left. - A\sigma_{g'}^2 - A\sigma_{\mathrm{ix}}^2 + \sigma_{g'}^2 + \sigma_{\mathrm{ix}}^2\right)\right)\end{aligned} \tag{11}$$

This equation can be rewritten as

$$\tilde{i}_v = \frac{a_1 x}{a_3 + a_4 e^{-a_2 x^2}} \tag{12}$$

with $a_1 = A\sigma_{ix}$, $a_2 = \frac{\sigma_{ix}^2}{2\sigma_{g'}^2(\sigma_{g'}^2+\sigma_{ix}^2)}$, $a_3 = \frac{A(\sigma_{g'}^2+\sigma_{ix}^2)}{\sigma_{ix}}$, $a_4 = (1-A)(\sigma_{g'}^2 + \sigma_{ix}^2)\sqrt{1/\sigma_{g'}^2 + 1/\sigma_{ix}^2}$ and $x = r_v - \tilde{s}_v$. Note that a_1, a_2, a_3 and a_4 are constants that do not depend on x. The term $a_4 e^{-a_2 x^2}$ will change rapidly with x from much higher than a_3 to much lower than a_3 due to its exponential nature.

This implies that the expression can be simplified for large and small values of $|x| = |r_v - \tilde{s}_v|$. For large values, (11) is given by

$$\tilde{i}_v \approx \frac{\sigma_{\text{ix}}^2 (r_v - \tilde{s}_v)}{\sigma_{g'}^2 + \sigma_{\text{ix}}^2} \approx (r_v - \tilde{s}_v) \tag{13}$$

where the last approximation is valid as long as $\sigma_{\text{ix}}^2 \gg \sigma_{g'}^2$.

For small values of $|r_v - \tilde{s}_v|$ the result of the expression is much lower than $r_v - \tilde{s}_v$ and can be taken as zero. This can be seen by noting that if $z = a_4 e^{-a_2 x^2} \gg a_3$ then

$$\tilde{i}_v = \frac{a_1 x}{a_3 + z} \ll \frac{a_1 x}{a_3} = \frac{\sigma_{\text{ix}}^2 (r_v - \tilde{s}_v)}{\sigma_{g'}^2 + \sigma_{\text{ix}}^2} \approx (r_v - \tilde{s}_v) \tag{14}$$

Note, that due to the exponential term the value of the expression will change rapidly from one value to the other, in fact implementing a threshold function. This can be confirmed by plotting the function for a set of typical values of its parameters as done in Fig. 2.

The value of the transition from high to low can be calculated in the case of $\sigma_{\text{ix}}^2 \gg \sigma_{g'}^2$ by solving $\tilde{i}_v = (r_v - \tilde{s}_v)/2$ or making $a_3 = a_4 e^{-a_2 x^2}$, resulting in

$$t = \sigma_{g'} \sqrt{\log\left(\frac{\sigma_{\text{ix}}^2}{A^2 \sigma_{g'}^2}\right)}. \tag{15}$$

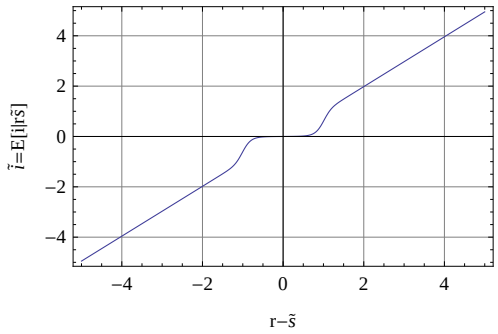

Figure 2: The MMSE estimate of i given $r = r_v$ and $\tilde{s} = \tilde{s}_v$, for $A = 0.1$, $\sigma^2_{g'} = 0.1$ and $\sigma^2_{\text{ix}} = 10$.

Finally, a simple intuitive explanation for the result obtained is given. The value of $r_v - \tilde{s}_v$ is an estimate for the total noise, Gaussian noise plus impulsive noise. If this estimate is low, $r_v - \tilde{s}_v < t$, then the sample is taken to be from Gaussian noise, and the estimate for i is zero. On the other hand, if the estimate is high, $r_v - \tilde{s}_v > t$, an impulse is detected and $\tilde{i}_v = r_v - \tilde{s}_v$.

4. Transform Domain Signal Estimate

The paper subsequently determines how to estimate the signal in the transform domain. Let $S(k)$, $R(k)$, $I(k)$ and $G(k)$ and their variants be the DFT of $s(n)$, $r(n)$, $i(n)$, $g(n)$ and variants, respectively, where n takes values from 0 to $2N-1$. The DFT is applied to vectors of length $2N$ formed by the time domain signals as in OFDM where N is the number of sub-carriers or tones since baseband transmission is assumed. In the transform domain, the noise component $G(k) + I(k)$ is taken to be Gaussian. This is justified by the central limit theorem, since the noise at any given frequency is formed by the contribution of many independent noise sources (the samples in the

time domain). First we calculate $P(S|\tilde{I}, R)$ where $\tilde{I}_v$ is the current estimate of I and the dependence of k was dropped. The noise components are also taken to be uncorrelated because the DFT approximately diagonalize typical Toeplitz autocorrelation matrices in the time domain. Following a similar approach to the time domain impulsive noise estimation, one has

$$P(S|\tilde{I}, R) = \frac{P(S)P(G' = R_v - \tilde{I}_v - S_v)}{\iint_{-\infty}^{\infty} P(S)P(G' = R_v - \tilde{I}_v - S_v)d^2S_v} \tag{16}$$

where G' is a Gaussian random variable with variance, $\sigma^2_{G'} = \sigma^2_G + \sigma^2_{\tilde{I}}$, the sum of the variance of $G(k)$ plus the variance of the transform domain impulse estimate, $\tilde{I}$. The PDF of S corresponds to that of a QAM or PSK signal constellation. This results in

$$P(S|\tilde{I}, R) = \frac{\sum_{X\in\mathcal{X}} \delta(S_v - X)\mathrm{PDF}_{\mathrm{CN}}(R_v, \tilde{I}_v + X, \sigma^2_{G'})}{\sum_{X\in\mathcal{X}} \mathrm{PDF}_{\mathrm{CN}}(R_v, \tilde{I}_v + X, \sigma^2_{G'})} \tag{17}$$

and in

$$\tilde{S}_v = \mathrm{E}[S|\tilde{I}, R] = \frac{\sum_{X\in\mathcal{X}} X\,\mathrm{PDF}_{\mathrm{CN}}(R_v, \tilde{I}_v + X, \sigma^2_{G'})}{\sum_{X\in\mathcal{X}} \mathrm{PDF}_{\mathrm{CN}}(R_v, \tilde{I}_v + X, \sigma^2_{G'})} \tag{18}$$

where $\mathrm{PDF}_{\mathrm{CN}}(X, M, \sigma^2)$ is the PDF of the complex Gaussian distribution with mean M and variance σ^2, and $\mathcal{X}$ is the set of the points in the QAM or PSK constellation.

The MMSE estimator of S is given by (18) while the MAP estimator is given by maximizing (17) with respect to S_v. This will result in the simple QAM/PSK demodulator that selects the closest point in the constellation to the received signal, and which is typically implemented by simply rounding the received signal after subtracting the current noise estimate. The received signal minus the current noise estimate is referred to as $\tilde{R}_v(k) = R_v(k) - \tilde{I}_v(k)$. The estimate of S is referred to as $\tilde{S}_v$ in both cases.

5. Implementation

In this paper, we propose two implementations of the proposed technique. Both use the MAP estimator in the transform domain because it is difficult to obtain an estimate for σ'_G which is required for the MMSE transform domain S estimator. In the case of the time domain impulse estimator, obtaining an estimate for σ'_g is required. In both of our implementations this estimate is given by the sample variance for known mean

$$\sigma^2_{g'} \approx \text{s\_var}(r_v - \tilde{s}_v - \tilde{\tilde{i}}_v) := \sum_{n=0}^{2N-1} \frac{(r_v(n) - \tilde{s}_v(n) - \tilde{\tilde{i}}_v(n))^2}{2N} \tag{19}$$

where $\tilde{\tilde{i}}_v$ is the estimate of i obtained in the previous iteration of the technique, and the calculation is repeated for each iteration of the technique.

Technique I uses the exact MMSE estimate given by (11). Technique II uses a hard threshold impulse estimator, with the threshold t, namely

$$\tilde{\tilde{i}}_v = \begin{cases} r_v - \tilde{s}_v & \text{if } |r_v - \tilde{s}_v| > t \\ 0 & \text{if } |r_v - \tilde{s}_v| \leq t \end{cases} \tag{20}$$

Also, Technique I has A and σ_{ix} as parameters, while Technique II has a single parameter, K, so that the impulse detection threshold, t, is given by $t = \sigma_{g'} K$; where K can also be calculated from A, σ_{ix} and $\sigma_{g'}$ using (15). Note that K is not very sensitive to variations in these parameters because of the log function in (15) so it can be taken as constant. Technique II is very similar to the technique proposed by Zhidkov [9]. The only difference is that in [9] $\sigma^2_{g'} \approx \text{s\_var}(r_v - \tilde{s}_v)$. However, in this paper we offer a strong theoretical base for the technique and effective formulas for the calculation of K, while [9] does not have a theoretical foundation.

The resulting technique is presented in Technique 1. Regarding the computation complexity of Technique II it is dominated by the calculations of the fast fourier transform (FFT) and is equal to $(1 + 2 \times n)$ FFTs where n is the number of iterations of the technique.

Algorithm 1 - Proposed Technique I and II

1: Calculate the DFT of the received signal (as in OFDM).
2: **for** j=1 to number of iterations **do**
3: Subtract the current impulsive noise estimate from the received signal ($\tilde{R}_v(k) = R_v(k) - \tilde{I}_v(k)$).
4: MAP signal estimate: estimate the transmitted signal using QAM demodulation. ($\tilde{S}_v(k) = \text{QAM\_demodulation}(\tilde{R}_v(k))$)
5: **if** reached last iteration **then**
6: stop
7: **end if**
8: Calculate the IDFT of the transmitted signal estimate ($\tilde{s}_v(n) = \text{IDFT}(\tilde{S}_v(k))$, where k goes from 0 to $2N - 1$).
9: Calculate the estimate of the variance of the Gaussian noise ($\sigma^2_{g'}$) using the variance of the total noise estimate minus the current impulsive noise estimate, equation (19).
10: MMSE Impulsive Noise Estimate: estimate the time domain impulsive noise using: Technique I - equation (11); Technique II equation (20), using the threshold given by (15). (calculate $\tilde{i}_v(n)$)
11: Calculate the DFT of the impulsive noise estimate ($\tilde{I}_v(k) = \text{DFT}(\tilde{i}_v(n))$, where n goes from 0 to $2N - 1$).
12: **end for**

6. Multi-path Channel

The techniques presented above needs to be slightly modified in order to deal with non-ideal channel, but the modification is straightforward. We add zero forcing channel equalization after applying the DFT corresponding to multiplying by $H^{-1}(k)$, as in classical OFDM; and add inverse channel equalization ($H(k)$) before applying the inverse DFT (IDFT). This results in the technique presented in Fig. 3.

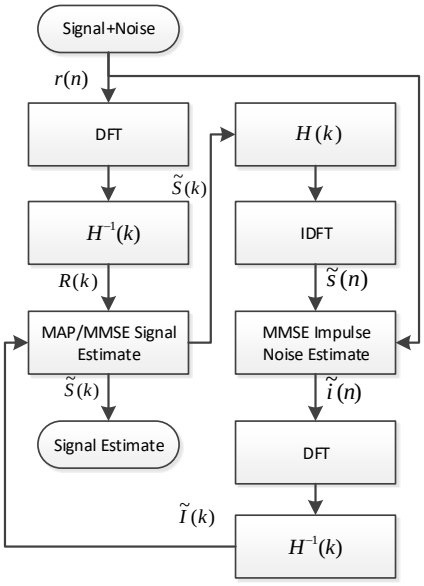

Figure 3: The proposed technique modified to use with a multi-path channel.

7. Simulation Results

This section presents simulation results comparing techniques I and II with the technique proposed by Zhidkov in [9]. In Zhidkov's technique, the parameter that selects the impulse detection threshold was set to $C = 5$,

determined experimentally to minimize the probability of bit error (P_b). In Technique I, the parameters A and σ_{ix} were set to the theoretical values, and in Technique II the parameter was set to $K = 3$, calculated based on typical values of the impulsive noise parameters.

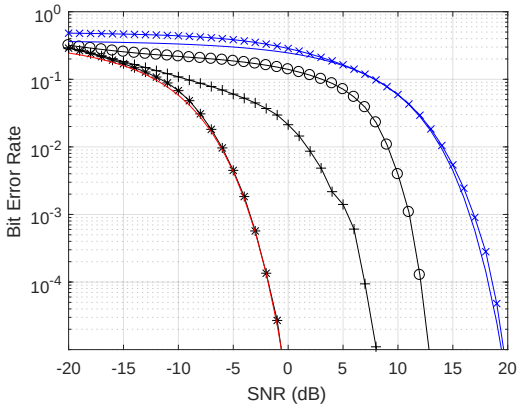

Figure 4: Bit error rate of the Proposed Technique version II with 16-QAM, A=0.01, N=1024, T=100, and different number of iterations. The lines without markers are the theoretical curves in the case of no impulsive noise reduction (blue) and full impulse removal (red). The $\times$ maker is for the experimental line for no impulsive noise reduction; $\bigcirc$ is with two iterations, $+$ is 5 iterations and $*$ is 10 iterations.

In Fig. 4 P_b is plotted for a 16-QAM modulation using the Proposed Technique II, versus the signal to noise ratio (SNR) for Middleton class A noise. Note that the SNR is the SNR at the receiver, without impulsive noise removal, so it is the power of the signal divided by the power of the Gaussian plus impulsive noise. Removing the impulses improves the performance implying that low error rates are possible at low SNR, much better than in the Gaussian noise case.

The parameter T is $T = \sigma_i^2/\sigma_g^2$. In these simulations, impulses are fairly

rare ($A = 0.01$) but large, making it possible to achieve almost complete impulsive noise removal. This can be seen in Fig. 4 since the line corresponding to 10 iterations overlaps the line for the theoretical value of P_b when there is no impulsive noise.

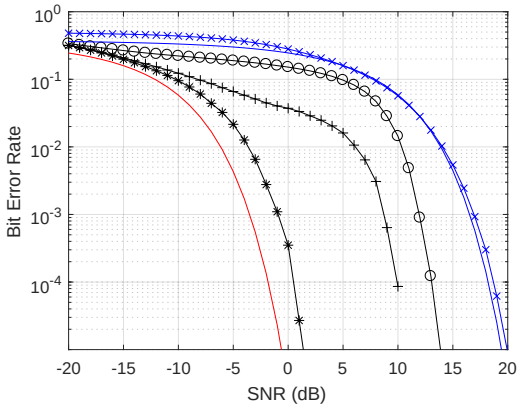

Figure 5: Bit error rate of the Zhidkovs technique with 16-QAM, A=0.01, N=1024, T=100, and different number of iterations. The lines without markers are the theoretical curves in the case of no impulsive noise reduction (blue) and full impulse removal (red). The $\times$ maker is for the experimental line with no impulsive noise reduction; $\bigcirc$ is with two iterations, $+$ is 5 iterations and $*$ is 10 iterations.

Fig. 5 is the same plot as Fig. 4 but for Zhidkov's technique. It can be seen that the technique performance improves with the number of iterations but it does not reach the same performance, close to complete impulsive noise removal as in Proposed Technique II.

Fig. 6 compares the performance of Zhidkov's and the Proposed Technique I and II for $A = 0.1$. It shows that all the techniques have a similar performance, close to 4 dB of SNR gain for $P_b = 10^{-2}$. The Proposed Technique I has slightly lower performance than the others. This may be because

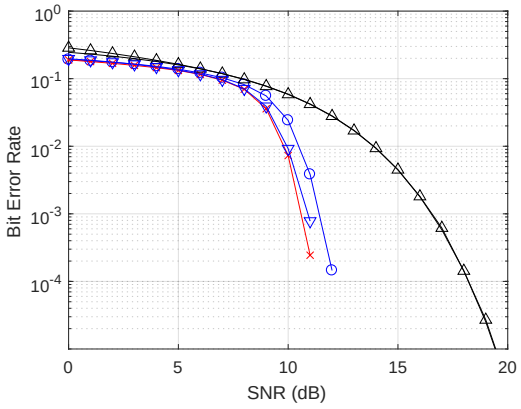

Figure 6: Comparing Zhidkov's technique and Proposed Technique I and II with 16-QAM, $A = 0.1$, $N = 1024$, $T = 100$, 5 iterations. Black $\triangle$ is no noise reduction; blue $\bigcirc$ and ∇ is Proposed I and II and red $\times$ is Zhidkov.

its parameters were chosen using theoretical values, instead of being fine-tuned to achieve the best performance.

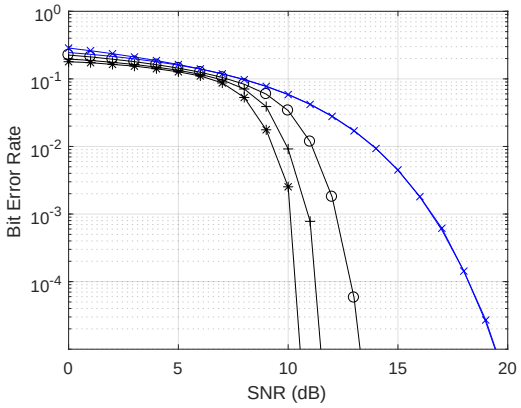

Figure 7: The Proposed Technique version II with 16-QAM, A=0.1, N=1024, T=100, and different number of iterations. The blue $\times$ line is no impulsive noise; black $\bigcirc$ is with two iterations, $+$ is 5 iterations and $*$ is 10 iterations.

Fig. 7 is similar to Fig. 4 but using more frequent (and smaller for the

same SNR) impulses, $A = 0.1$. It can be seen that it is no longer possible to achieve complete impulsive noise removal, and that the SNR gain is about 5 dB for $P_b = 10^{-2}$ for 10 iterations.

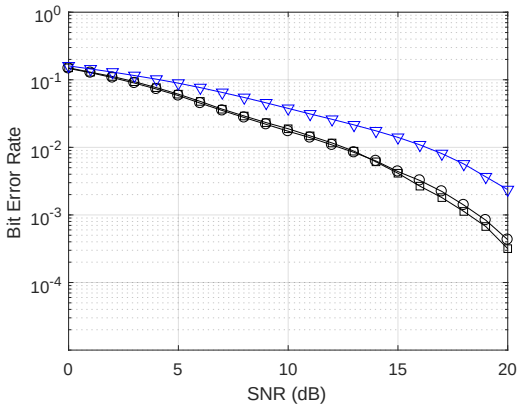

Figure 8: Bit error rate of the Proposed Technique version II and Zhidkovs technique with 16-QAM, and measured noise using 10 iterations. Blue ∇ is no noise reduction; black $\bigcirc$ is Zhidkovs technique and $\square$ is the Proposed Technique II.

In Fig. 8 the Proposed Technique II and Zhidkovs technique are tested using measured power lines noise [22, 23] filtered to a 20 MHz bandwidth and with a 40 MHz sample rate. This noise was recorded directly from power line plugs in our university in an office building during work hours. This noise is characterized by impulses with a relative long duration, a bit more like bursts much like the noise described in [4]. One notes that both techniques have very similar performance, achieving a SNR gain of about 4 dB for $P_b = 10^{-2}$.

Finally, Fig. 11 shows the performance of the Proposed Technique in a multi-path channel. The channel model used was the proposed in [24] for the power line channel [3], with parameters $g = 0.01$, $a_0 = 0$, $a_1 = 2\,\mathrm{dBMHz}^{-1}m^{-1}$, $k = 1$ and 10 paths with lengths ranging from $50\,m$ to $320\,m$

and a sample rate of 40 MHz. The resulting frequency response is plotted in Fig. 9. Circular prefix add and removal was assumed (but not actually implemented), resulting in a channel just characterized by the frequency and phase response at each frequency.

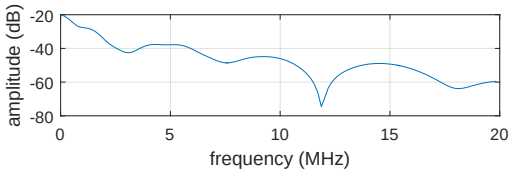

Figure 9: Frequency response of the multi-path channel used in the simulations.

Adaptive modulation was used as described in [25, sec. VII], resulting in the bit allocation presented in Fig. 10. Then this bit allocation was fixed and the transmitted power was changed resulting in varying SNR and bit error probability as plotted in Fig. 11. The number of iterations of the algorithm was 10.

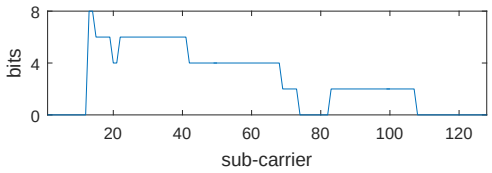

Figure 10: Number of bits allocated to each carrier after bit loading.

Fig. 11 shows that the Proposed Technique has a performance improvement of as much as 8 dB SNR over the a MODEM without any impulse removal and only loses 2.4 dB to a MODEM that is able to perfectly remove all the impulses; for $P_b = 10^{-3}$ and the parameters of the simulation in the figure.

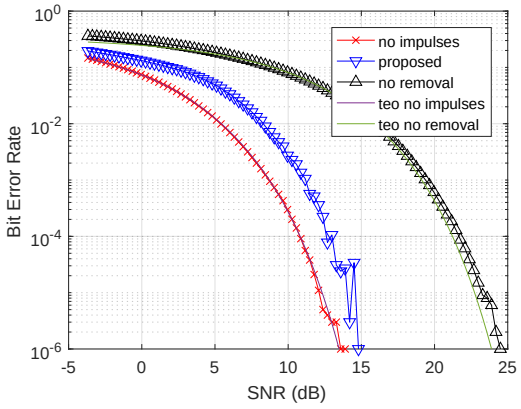

Figure 11: Performance of the Proposed Technique on a multi-path channel. The line named no impulses represents the performance of a MODEM were the impulsive noise is completely removed. The line named no removal represents a naive MODEM that does not remove impulsive noise. The lines with "teo" in the name represent the theoretical calculated values for the the corresponding MODEMs. The impulsive noise had parameters A=0.1 and T=10. The OFDM system had 128 carriers modulated as presented Fig. 10.

8. Conclusions

In this paper, we derive an iterative MMSE/MAP impulsive noise reduction technique for OFDM communications. The technique works as follows: i) obtain an MMSE/MAP estimate for the signal in the transform domain; ii) use this estimate to make an MMSE estimate of the impulsive noise in the time domain; iii) use this estimate to refine the signal estimate in the transform domain; repeat for a predetermined number of times. It is shown that MMSE impulse estimation in the time domain is approximately equal to detecting the impulses by comparing the signal with a threshold. An expression for this threshold value was determined. The proposed techniques are similar to previous works, but, comparing with the work of Haring the

solution is simplified. When comparing with the work of Zhidkov, we give a stronger theoretical foundation, and a new variance estimate. The technique was tested with simulated Middleton noise and measured noise from power lines resulting in a performance similar to Zhidkovs technique.

9. Acknowledgements

This work was supported by national funds through Fundação para a Ciência e a Tecnologia (FCT) with reference UID/CEC/50021/2013.

10. References

[1] T. Shongwey, A. Vinck, H. C. Ferreira, On impulse noise and its models, in: 18th IEEE International Symposium on Power Line Communications and its Applications (ISPLC), 2014, pp. 12–17.

[2] D. Middleton, I. of Electrical, E. Engineers, An introduction to statistical communication theory, Vol. 960, McGraw-Hill New York, 1960.

[3] M. Gotz, M. Rapp, K. Dostert, Power line channel characteristics and their effect on communication system design, IEEE Communications Magazine 42 (4) (2004) 78–86.

[4] M. Zimmermann, K. Dostert, Analysis and modeling of impulsive noise in broad-band powerline communications, IEEE transactions on Electromagnetic compatibility 44 (1) (2002) 249–258.

[5] S. V. Zhidkov, Performance analysis and optimization of OFDM receiver with blanking nonlinearity in impulsive noise environment, Vehicular Technology, IEEE Transactions on 55 (1) (2006) 234–242.

[6] S. V. Zhidkov, Analysis and comparison of several simple impulsive noise mitigation schemes for OFDM receivers, IEEE Transactions on Communications 56 (1) (2008) 5–9.

[7] D.-F. Tseng, Y. S. Han, W. H. Mow, L.-C. Chang, A. H. Vinck, Robust clipping for OFDM transmissions over memoryless impulsive noise channels, IEEE Communications Letters 16 (7) (2012) 1110–1113.

[8] M. Korki, N. Hosseinzadeh, T. Moazzeni, Performance evaluation of a narrowband power line communication for smart grid with noise reduction technique, IEEE Transactions on consumer electronics 57 (4).

[9] S. V. Zhidkov, Impulsive noise suppression in OFDM-based communication systems, Consumer Electronics, IEEE Transactions on 49 (4) (2003) 944–948.

[10] J. Haring, A. H. Vinck, Iterative decoding of codes over complex numbers for impulsive noise channels, Information Theory, IEEE Transactions on 49 (5) (2003) 1251–1260.

[11] G. Caire, T. Y. Al-Naffouri, A. K. Narayanan, Impulse noise cancellation in OFDM: an application of compressed sensing, in: IEEE International Symposium on Information Theory (ISIT 2008), 2008, pp. 1293–1297.

[12] P. A. Lopes, J. A. Gerald, Improving bit error rate under burst noise in OFDM power line communications, Digital Signal Processing 51 (2016) 47–53.

[13] Y.-R. Chien, Iterative channel estimation and impulsive noise mitigation algorithm for OFDM-based receivers with application to power-line

communications, IEEE Transactions on Power Delivery 30 (6) (2015) 2435–2442.

[14] M. Korki, J. Zhang, C. Zhang, H. Zayyani, Block-sparse impulsive noise reduction in OFDM systemsa novel iterative bayesian approach, IEEE Transactions on Communications 64 (1) (2016) 271–284.

[15] M. Nassar, P. Schniter, B. L. Evans, A factor graph approach to joint OFDM channel estimation and decoding in impulsive noise environments, IEEE Transactions on Signal Processing 62 (6) (2014) 1576–1589.

[16] J. Lin, M. Nassar, B. L. Evans, Impulsive noise mitigation in powerline communications using sparse bayesian learning, IEEE Journal on Selected Areas in Communications 31 (7) (2013) 1172–1183.

[17] T. Y. Al-Naffouri, A. A. Quadeer, G. Caire, Impulse noise estimation and removal for OFDM systems, IEEE Transactions on Communications 62 (3) (2014) 976–989.

[18] D. H. Sargrad, J. W. Modestino, Errors-and-erasures coding to combat impulse noise on digital subscriber loops, IEEE transactions on communications 38 (8) (1990) 1145–1155.

[19] T. Faber, T. Scholand, P. Jung, Turbo decoding in impulsive noise environments, Electronics letters 39 (14) (2003) 1069–1071.

[20] H. Nakagawa, D. Umehara, S. Denno, Y. Morihiro, A decoding for low density parity check codes over impulsive noise channels, in: IEEE International Symposium on Power Line Communications and Its Applications, 2005, pp. 85–89.

[21] P. Billingsley, Probability and measure. wiley series in probability and mathematical statistics, Wiley New York, 1995.

[22] P. A. Lopes, J. M. Pinto, J. B. Gerald, Dealing with unknown impedance and impulsive noise in the power-line communications channel, Power Delivery, IEEE Transactions on 28 (1) (2013) 58–66.

[23] P. A. Lopes, J. A. Gerald, Power line noise measurements data (2010). URL `http://web.tecnico.ulisboa.pt/paulo.lopes/PLCNoise/`

[24] M. Zimmermann, K. Dostert, A multipath model for the powerline channel, IEEE Transactions on communications 50 (4) (2002) 553–559.

[25] P. A. Lopes, J. M. Pinto, J. B. Gerald, Modeling and optimization of the access impedance of power line channels, in: IEEE International Symposium on Power Line Communications and Its Applications (ISPLC 2010), 2010, pp. 142–147.